

## Bivalent Ligands of CXCR4 with Rigid Linkers for Elucidation of the Dimerization State in Cells

Tomohiro Tanaka, Wataru Nomura,\* Tetsuo Narumi, Akemi Masuda, and Hirokazu Tamamura\*

Department of Medicinal Chemistry, Institute of Biomaterials and Bioengineering, Tokyo Medical and Dental University, 2-3-10 Kandasurugadai, Chiyoda-ku, Tokyo 101-0062, Japan

Received August 18, 2010; E-mail: nomura.mr@tmd.ac.jp; tamamura.mr@tmd.ac.jp

**Abstract:** To date, challenges in the design of bivalent ligands for G protein-coupled receptors (GPCRs) have revealed difficulties stemming from lack of knowledge of the state of oligomerization of the GPCR. The synthetic bivalent ligands with rigid linkers that are presented here can predict the dimer form of CXCR4 and be applied to molecular probes in cancerous cells. This “molecular ruler” approach would be useful in elucidating the details of CXCR4 oligomer formation.

The chemokine receptor CXCR4 is a membrane protein belonging to the family of G protein-coupled receptors (GPCRs). In current drugs, ~60% of drug target molecules are located at the cell surface, and half of them are GPCRs.<sup>1</sup> Recent studies have indicated a pivotal role for homo- and heterooligomerization of CXCR4 in cancer metastasis, and the significance of oligomeric forms of GPCR has been gaining acceptance.<sup>2</sup> However, the functional implications proposed for these oligomers, which include signal transduction and internalization, are poorly understood and require additional studies.<sup>3</sup> Efforts to understand those correlations have used photochemical analyses such as bioluminescence resonance energy transfer (BRET) analysis,<sup>3,4</sup> but the elucidation of the native state of CXCR4 in living cells is complicated by conformational or functional changes resulting from mutations. Estimates of the precise distance between ligand binding sites in the dimer form would permit the development of bivalent ligands of CXCR4 having improved binding affinity and specificity.<sup>5</sup> In spite of the enormous effort devoted to the design of bivalent ligands, rational design of such linkers has been difficult because of the lack of knowledge concerning the dimeric form of GPCRs. Therefore, there is an increasing demand for a novel strategy for the analysis of the precise distance between ligand binding sites.<sup>6</sup>

In this study, we designed and synthesized novel CXCR4 bivalent ligands consisting of two molecules of an FC131<sup>7</sup> analogue, [*cyclo*(D-Tyr-Arg-Arg-Nal-D-Cys-)] [Nal = L-3-(2-naphthyl)alanine, **1a**], connected by a poly(L-proline) or a PEGylated poly(L-proline) linker. Poly(L-prolines) have been utilized as rigid linkers between the two functional units, which require a predetermined separation for activity.<sup>8</sup> Linkers consisting of poly(L-prolines) were expected to maintain constant distances of 2–8 nm between the ligands. Our bivalent ligands with linkers of various lengths were used to determine the distance between two binding sites of ligands consisting of CXCR4 dimers. Acetamide-capped FC131 (**1b**), in which Gly is replaced by D-Cys and the thiol group of Cys is capped with an acetamide group, was synthesized as a monomer unit of the ligand (Figure 1). Although this substitution caused a 2-fold decrease in binding to CXCR4, the binding affinity was still adequate for analyses. Poly(L-proline) helices are known to maintain a length of 0.9 nm per turn.<sup>9</sup> In this study, polyproline- and

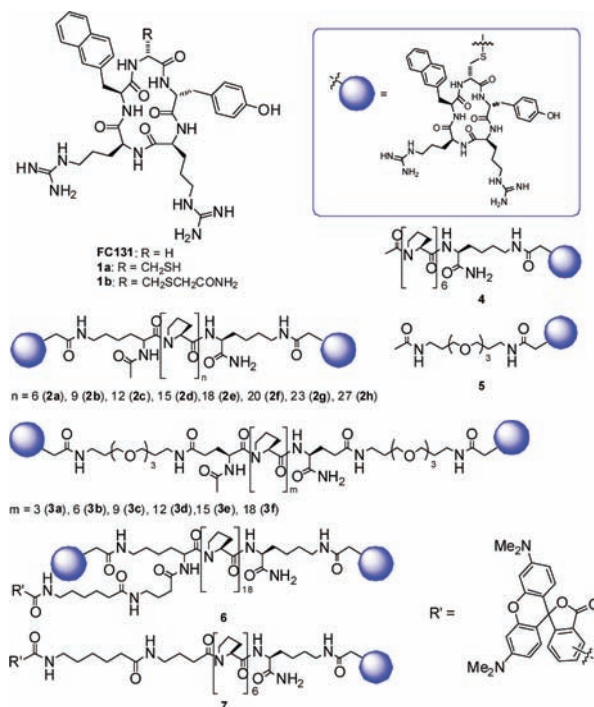


**Figure 1.** Design of bivalent ligands against chemokine receptor CXCR4. As CXCR4 binding moieties, D-Cys FC131 (R = CH<sub>2</sub>SH, **1a**) and acetamide-capped FC131 (R = CH<sub>2</sub>SCH<sub>2</sub>CONH<sub>2</sub>, **1b**) were prepared. Poly(L-proline) (**2a–h**) and PEG-conjugated poly(L-proline) (**3a–f**) with CXCR4 binding moieties on both ends were synthesized. As monomer binding ligands with linkers, Ac6pro FC131 (**4**) and AcPEG FC131 (**5**) were synthesized. Tetramethylrhodamine (TAMRA)-labeled **2e** (**6**) and **4** (**7**) were prepared for the imaging experiments.

PEGylated polyproline-type linkers with lengths of 2–8 nm were synthesized.<sup>10</sup> The synthetic linkers and their conjugated bivalent ligands were characterized by high-resolution mass spectrometry (HRMS) (Tables S3 and S5 in the Supporting Information), and their CD spectra clearly showed the presence of a type-II polyproline helix (Figure S3 in the Supporting Information). As monomer controls, FC131 analogues **4** and **5** with hexaproline and poly(ethylene glycol) (PEG) linkers, respectively, that were acetylated at the other end were also prepared.

The binding affinities of the synthetic ligands were evaluated in a competitive binding assay against [<sup>125</sup>I]-SDF-1α, as reported previously.<sup>7d</sup> The binding assay showed that the binding affinity of our bivalent ligands is clearly dependent on the linker length. Ligands of the poly(L-proline) type with the highest affinities were **2e** and **2f**. Among the PEGylated poly(L-proline)-type ligands, **3c** and **3d** showed the highest affinity. The linker-optimized bivalent ligands, **2f** and **3d**, showed 7.3- and 21-fold increases in binding affinity relative to **4** and **5**, respectively (Table 1). These results

**Table 1.** Summary of Binding Affinities of Synthetic Bivalent and Monovalent Ligands Analyzed by [<sup>125</sup>I]-SDF-1 $\alpha$  Competition Assay

compd	K <sub>i</sub> (nM) <sup>a</sup>	linker length (nm)	compd	K <sub>i</sub> (nM) <sup>a</sup>	linker length (nm)
FC131	31.5	—	<b>3a</b>	87.2	3.8
<b>1b</b>	53.4	—	<b>3b</b>	45.6	4.7
<b>2a</b>	51.2	1.8	<b>3c</b>	17.8	5.6
<b>2b</b>	45.4	2.7	<b>3d</b>	13.9	6.5
<b>2c</b>	64.4	3.6	<b>3e</b>	49.3	7.4
<b>2d</b>	59.5	4.5	<b>3f</b>	83.3	8.3
<b>2e</b>	13.2	5.4	<b>4</b>	72	—
<b>2f</b>	9.9	6	<b>5</b>	294	—
<b>2g</b>	22.5	6.9	<b>7</b>	119	—
<b>2h</b>	45.8	8.1			

<sup>a</sup> K<sub>i</sub> values are the concentrations corresponding to 50% inhibition of [<sup>125</sup>I]-SDF-1 $\alpha$  binding to Jurkat cells.

indicate successful bivalent binding of the ligands, which has been known to be responsible for an increase in binding affinity.<sup>5a</sup> It should be noted that the maximum increase in binding affinity was observed for ligands of the two linker types having similar lengths (5.5–6.5 nm). In the dimer state of CXCR4, there are several forms of assembly (head-to-head, tail-to-tail, and head-to-tail).<sup>5a</sup> These forms have different distances between the binding sites of the ligands. Molecular modeling studies of FC131 with CXCR4 suggested that amino acids in transmembrane (TM) 7 are important for FC131 binding.<sup>11</sup> Through the use of the rhodopsin structure, it was revealed that in the TM 4 and 5 assembly form, the linear distance between ligand binding sites is 5.3 nm. In the other forms of possible assembly, the linear distances were determined to be 3.5 and 3.9 nm for TM 1 and 2 assembly and the combination of TM 1–4 and TM 2–5 assembly, respectively (Figure S4). The changes in binding affinity were relatively moderate, and although the existence of different assembly forms is possible, a majority of the population should be in the TM 4 and 5 assembly form.

From the increased binding affinity of linker-optimized bivalent ligands, a hypothesis was derived that such ligands could be applied as probes specific to CXCR4 on the cell surface because the receptors are overexpressed in several kinds of malignant cells<sup>12</sup> and that the dimer formation of the receptor should depend on the expression level. Accordingly, compound **2e**, which showed high binding affinity, was chosen for labeling with tetramethylrhodamine (TAMRA) and applied to the imaging of CXCR4. The TAMRA moiety was conjugated to an N-terminal of the proline linker via  $\gamma$ -butyric acid. To confirm that the ligands specifically bind to CXCR4, a CXCR4–EGFP fusion protein (EGFP = enhanced green fluorescent protein) was transiently expressed in HeLa cells. The increase in binding affinity of the bivalent ligand was clearly reflected in the imaging of CXCR4, as a merged image of TAMRA-labeled **2e** (**6**) and EGFP-fused CXCR4 was observed (Figure 2). When a control monomer, TAMRA-labeled **4** (**7**), was utilized for detection, only a trace of binding was observed. Additionally, binding to mock HeLa cells at the same concentration of ligands was not observed for either ligand (Figure S5).

To further evaluate the binding specificity and dependence on CXCR4 expression levels, fluorescence-activated cell sorting (FACS) analyses utilizing Jurkat, K562, and HeLa cells were performed (Figure 3). The cells were adopted on the basis of their different levels of CXCR4 expression (Jurkat > HeLa > K562).<sup>13</sup> The binding was evaluated by changes in mean fluorescence intensity (MFI) of the above cells in the presence and absence of ligands. The bivalent ligand **6** showed intense binding to Jurkat cells, which highly express CXCR4, as evidenced by the 2.3- and 3.3-fold increases in MFI at 25 and 250 nM, respectively. For binding to HeLa cells, the MFI was increased 2.4-fold by binding

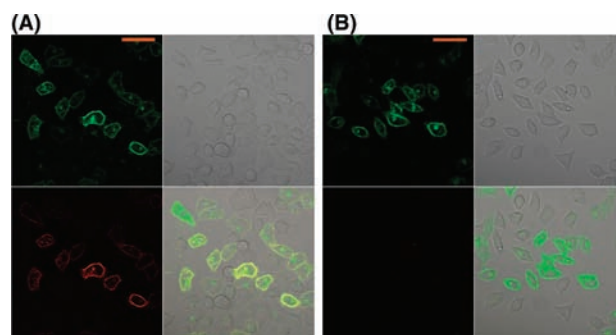


**Figure 2.** Binding of TAMRA-labeled FC131-derived monovalent and bivalent ligands to EGFP–CXCR4-transfected HeLa cells. Bivalent ligand **6** with an optimized linker length was utilized. The pictures show the binding of (A) **6** (25 nM) and (B) **7** (50 nM). Each panel is divided into four sections as follows: upper left, EGFP emission; upper right, differential interference contrast (DIC) image; lower left, TAMRA emission conjugated to ligands; lower right, merged image. Orange bars in the panels represent 50  $\mu$ m.

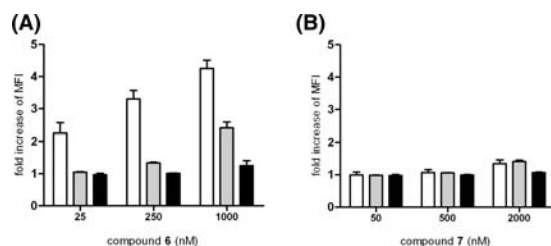


**Figure 3.** FACS analysis to evaluate the dependence of ligand binding on the levels of CXCR4 expression. The columns show the binding of (A) **6** and (B) **7** to Jurkat (white), HeLa (gray), and K562 (black) cells. The fold increase values were calculated by dividing the MFIs of the above cells in the presence of ligands by the corresponding values in the absence of ligands. The results are means of three independent experiments; error bars indicate standard errors of the mean.

of ligand **6** at 1  $\mu$ M, although no significant increase in MFI was observed at 25 or 250 nM **6**, which corresponds with the imaging experiment (Figure S5). Meanwhile, the monovalent ligand **7** at 2  $\mu$ M showed similar binding to Jurkat and HeLa cells, involving 1.1- and 1.4-fold increases in MFI, respectively. These results suggest that it is difficult to distinguish the expression level of CXCR4 by molecular imaging using the monovalent ligand. On the other hand, it is of special interest that the bivalent ligand showed distinguishability of the differences in CXCR4 expression levels. Furthermore, the binding of our CXCR4 ligands would be responsive to CXCR4, as no binding of either ligand to K562 cells, which express a trace of CXCR4, was observed. These results provide evidence in support of the hypothesis that the bivalent ligand binds preferentially to the constitutive dimer of CXCR4. Molecular imaging of CXCR4 on the cell surface by specific antibodies, such as c8352<sup>14</sup> or the monomer ligand T140,<sup>15</sup> has been previously reported. In the present system, however, it is possible that the bivalent ligands could distinguish the density of CXCR4 on the cell surface.

To further assess whether our bivalent ligand could distinguish between cancerous and normal cells by the imaging method, A549 and Human Umbilical Vein Endothelial Cells (HUVEC) were employed for staining as adhesive cell lines. A549 cells are human lung adenocarcinoma human alveolar basal epithelial cells, which are known to possess high CXCR4 expression levels.<sup>16</sup> HUVEC were chosen as a normal cell line without CXCR4 expression. It has been reported that the expression of CXCR4 on HUVEC is induced by fibroblast growth factor (FGF), which is highly expressed in the embryonic stage.<sup>17</sup> Thus, HUVEC was cultured

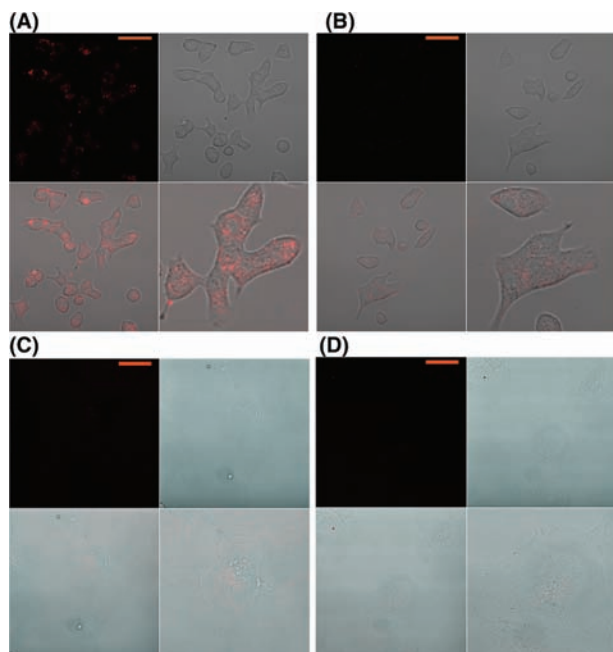


**Figure 4.** Imaging of CXCR4 by TAMRA-labeled FC131-derived monovalent and bivalent ligands on cancerous and normal primary cells. The panels show the binding of (A) **6** ( $1\ \mu\text{M}$ ) and (b) **7** ( $2\ \mu\text{M}$ ) to A549 cells and (C) **6** ( $250\ \text{nM}$ ) and (D) **7** ( $500\ \text{nM}$ ) to HUVEC cells. Each panel is divided into four sections as follows: upper left, TAMRA emission image; upper right, DIC image; lower left, merged image; lower right, focused image. Orange bars in the panels represent  $50\ \mu\text{m}$ .

in the absence of FGF. Ligand **6** showed clear binding to A549 cells (Figure 4A) but not to HUVEC (Figure 4C) at concentrations of  $1\ \mu\text{M}$  and  $250\ \text{nM}$ , respectively. On the other hand, monomer ligand **7** showed a trace of binding to each cell line (Figure 4B,D). Bivalent ligand **6** showed binding to HUVEC cultured with FGF at  $250\ \text{nM}$  (Figure S7). Thus, the bivalent ligands can detect cancerous cells that are in a state of high CXCR4 expression in a specific manner.

In summary, we have presented experimental results concerning the elucidation of the native state of the CXCR4 dimer utilizing bivalent ligands. These lead to a more precise understanding of the oligomerization state. Such a “molecular ruler” approach could be utilized in the design of bivalent ligands for any GPCR. It has been suggested that several GPCRs also exist as heterodimer forms, and CXCR4 has been hypothesized to form heterodimers with CCR2,<sup>18</sup> CCR5,<sup>19</sup> CXCR7,<sup>4b</sup> and the  $\delta$ -opioid receptor.<sup>20</sup> Although the biological significance of GPCRs in homo- or heterooligomerization is still unclear and controversial, the approach described here involving rigid linkers conjugated to ligands specific to each GPCR would lead to elucidation of these issues. Furthermore, through the avidity shown as the specific binding affinity for the dimeric form of CXCR4, the fluorescent-labeled bivalent ligands have been shown to be powerful tools for cancer diagnosis on the basis of their ability to distinguish the density of CXCR4 on the cell surface. Our approach has the advantages that the ligand can directly capture dimeric forms of GPCRs and that the linkers can be applied to virtually any known GPCR.

**Acknowledgment.** The authors thank Prof. Kazunari Akiyoshi (Tokyo Medical and Dental University) for access to the laser scanning microscope. T.T. was supported by JSPS Research Fellowships for Young Scientists. This research was supported in part by New Energy and Industrial Technology Development Organization (NEDO).

**Supporting Information Available:** Curve-fitting data for the binding analyses, CD spectra, docking study of bivalent ligand binding, imaging analyses of mock cells, histogram and MFI of FACS analysis, imaging analyses of HeLa cells cultured with FGF, experimental procedures, and spectral and analytical data for all new compounds. This material is available free of charge via the Internet at <http://pubs.acs.org>.

## References

- (1) Overington, J. P.; Al-Lazikani, B.; Hopkins, A. L. *Nat. Rev. Drug. Discovery* **2006**, *5*, 993–996.
- (2) Wang, J.; He, L.; Combs, C. A.; Roderiquez, G.; Norcross, M. A. *Mol. Cancer Ther.* **2006**, *5*, 2474–2483.
- (3) Percherancier, Y.; Berchiche, Y. A.; Slight, I.; Volkmer-Engert, R.; Tamamura, H.; Fujii, N.; Bouvier, M.; Heveker, N. *J. Biol. Chem.* **2005**, *280*, 9895–9903.
- (4) (a) Babcock, G. J.; Farzan, M.; Sodroski, J. *J. Biol. Chem.* **2003**, *278*, 3378–3385. (b) Luker, K. E.; Gupta, M.; Luker, G. D. *FASEB J.* **2009**, *23*, 823–834.
- (5) (a) Handl, H. L.; Sankaranarayanan, R.; Josan, J. S.; Vagner, J.; Mash, E. A.; Gillies, R. J.; Hruba, V. *J. Bioconjugate Chem.* **2007**, *18*, 1101–1109. (b) Zheng, Y.; Akgün, E.; Harikumar, K. G.; Hopson, J.; Powers, M. D.; Lunzer, M. M.; Miller, L. J.; Portoghese, P. S. *J. Med. Chem.* **2009**, *52*, 247–258.
- (6) Panetta, R.; Greenwood, M. T. *Drug Discovery Today* **2008**, *13*, 1059–1066.
- (7) (a) Tamamura, H.; Xu, Y.; Hattori, T.; Zhang, X.; Arakaki, R.; Kanbara, K.; Omagari, A.; Otaka, A.; Ibuka, T.; Yamamoto, N.; Nakashima, H.; Fujii, N. *Biochem. Biophys. Res. Commun.* **1998**, *253*, 877–882. (b) Fujii, N.; Oishi, S.; Hiramatsu, K.; Araki, T.; Ueda, S.; Tamamura, H.; Otaka, A.; Kusano, S.; Terakubo, S.; Nakashima, H.; Broach, J. A.; Trent, J. O.; Wang, Z.; Peiper, S. C. *Angew. Chem., Int. Ed.* **2003**, *42*, 3251–3253. (c) Tamamura, H.; Araki, T.; Ueda, S.; Wang, Z.; Oishi, S.; Esaka, A.; Trent, J. O.; Nakashima, H.; Yamamoto, N.; Peiper, S. C.; Otaka, A.; Fujii, N. *J. Med. Chem.* **2005**, *48*, 3280–3289. (d) Tanaka, T.; Tsutsumi, H.; Nomura, W.; Tanabe, Y.; Ohashi, N.; Esaka, A.; Ochiai, C.; Sato, J.; Itotani, K.; Murakami, T.; Ohba, K.; Yamamoto, N.; Fujii, N.; Tamamura, H. *Org. Biomol. Chem.* **2008**, *6*, 4374–4377.
- (8) (a) Arora, P. S.; Ansari, A. Z.; Best, T. P.; Ptashne, M.; Dervan, P. B. *J. Am. Chem. Soc.* **2002**, *124*, 13067–13071. (b) Sato, S.; Kwon, Y.; Kamisuki, S.; Srivastava, N.; Mao, Q.; Kawazoe, Y.; Uesugi, M. *J. Am. Chem. Soc.* **2007**, *129*, 873–880.
- (9) (a) Kuemin, M.; Schweizer, S.; Ochsenfeld, C.; Wennemers, H. *J. Am. Chem. Soc.* **2009**, *131*, 15474–15482. (b) Schuler, B.; Lipman, E. A.; Steinbach, P. J.; Kumke, M.; Eaton, W. A. *Proc. Natl. Acad. Sci. U.S.A.* **2005**, *102*, 2754–2759.
- (10) For synthesis details, see the Supporting Information.
- (11) Våbenø, J.; Nikiforovich, G. V.; Marshall, G. R. *Chem. Biol. Drug Des.* **2006**, *67*, 346–354.
- (12) Balkwill, F. *Semin. Cancer Biol.* **2004**, *14*, 171–178.
- (13) (a) Carnec, X.; Quan, L.; Olson, W. C.; Hazan, U.; Dragic, T. *J. Virol.* **2005**, *79*, 1930–1933. (b) Majka, M.; Rozmyslowicz, T.; Honczarenko, M.; Ratajczak, J.; Wasik, M. A.; Gaulton, G. N.; Ratajczak, M. *Z. Leukemia* **2000**, *14*, 1821–1832.
- (14) Schwartz, V.; Lue, H.; Kraemer, S.; Korbil, J.; Krohn, R.; Ohl, K.; Bucala, R.; Weber, C.; Bernhagen, J. *FEBS Lett.* **2009**, *583*, 2749–2757.
- (15) Nomura, W.; Tanabe, Y.; Tsutsumi, H.; Tanaka, T.; Ohba, K.; Yamamoto, N.; Tamamura, H. *Bioconjugate Chem.* **2008**, *19*, 1917–1920.
- (16) Murdoch, C.; Monk, P. N.; Finn, A. *Immunology* **1999**, *98*, 36–41.
- (17) Salcedo, R.; Wasserman, K.; Young, H. A.; Grimm, M. C.; Howard, O. M. Z.; Anver, M. R.; Kleinman, H. K.; Murphy, W. J.; Oppenheim, J. J. *Am. J. Pathol.* **1999**, *154*, 1125–1135.
- (18) Sohy, D.; Parmentier, M.; Springael, J. *J. Biol. Chem.* **2007**, *282*, 30062–30069.
- (19) Contento, R. L.; Molon, B.; Boullaran, C.; Pozzan, T.; Manes, S.; Marullo, S.; Viola, A. *Proc. Natl. Acad. Sci. U.S.A.* **2008**, *105*, 10101–10106.
- (20) Pello, O. M.; Martínez-Muñoz, L.; Parrillas, V.; Serrano, A.; Rodríguez-Frade, J. M.; Toro, M. J.; Lucas, P.; Monterrubio, M.; Martínez-A, C.; Mellado, M. *Eur. J. Immunol.* **2008**, *38*, 537–549.

JA107447W